

Plane strain elastoplastic consolidation of soil by finite elements II. Finite element inelastic consolidation analysis for a dike under wave action

S. PIETRUSZCZAK (WARSZAWA)

IN THE PAPER the finite element solution of an initial boundary-value problem is presented. The analysis concerns a dike standing on the subsoil and subjected to the cyclic action of waves during a storm. In particular, the dike at the mouth of the East Schelde river to the North Sea (Holland) is analysed and the numerical calculation simulates one of the in situ tests as performed in December 1975 on the prototype caisson. The presented solution is based upon the consolidation theory in which the saturated soil is treated as a multiphase medium. It is assumed that the soil skeleton is an elastoplastic material with isotropic hardening and the liquid phase is linearly compressible. The obtained finite element solution is compared with experimental measurements.

W pracy przedstawione jest rozwiązanie metodą elementów skończonych pewnego problemu początkowo-brzegowego. Analizowana jest zapora spoczywająca na podłożu gruntowym i poddana cyklicznemu działaniu fal w czasie sztormu. W szczególności analiza dotyczy zapory, która stanie u ujścia do Morza Północnego wschodniego odnóży rzeki Skaldy, natomiast obliczenia numeryczne symulują jeden z testów polowych przeprowadzonych w grudniu 1975 r. na prototypowym kesonie. Przedstawione rozwiązanie oparte jest na teorii konsolidacji, w której grunt traktowany jest ogólnie jako ośrodek wielofazowy. Założono, że ciecz jest liniowo ściśliwa, natomiast zachowanie szkieletu opisane jest przez model sprężysto-plastyczny z izotropowym wzmocnieniem. Wyniki otrzymane drogą numeryczną porównane są z pomiarami przeprowadzonymi w czasie testu.

В работе представлено решение с помощью метода конечных элементов некоторой начально-краевой задачи. Рассматривается плотина, покоящаяся на грунтовом основании и подверженная циклическому воздействию штормовых волн. В частности анализ относится к плотине, предусматриваемой в устье восточного рукава реки Скалды в Северное Море. Численный расчет моделирует одно из полевых испытаний проведенных в декабре 1975 года на прототипном кессоне.

1. Introduction

The aim of this paper is to present the finite element solution of an engineering initial, boundary-value problem. The analysed problem concerns the East Schelde dike subjected to the action of waves during a strong storm. The numerical calculations are directly connected with one of the in situ tests as performed on the prototype caisson in December 1975. The caisson was founded in the East Schelde estuary and loaded by a cyclically varying horizontal force which simulated the action of waves. In the numerical analysis we shall follow the loading history of this test and compare our results with experimental measurements.

During the test the real subsoil was remarkably saturated by water. The cyclic variations of loading caused cyclic changes in pore water pressure and this effect had a significant

influence upon the course of the deformation process. Therefore, the numerical analysis is based on the consolidation theory accounting for the multiphase nature of the soil mass. In particular, the computer program is constructed on the basis of the approach presented in the previous part of this paper [1]. In this approach the soil skeleton is assumed to be an elastoplastic isotropically hardening material. The model adopted for calculations is described in details in [1]. The water filling the pores is assumed to be linearly compressible and its movement is governed by Darcy's law.

The elastoplastic finite element solution is obtained by the "initial stress" approach as proposed by O. C. ZIENKIEWICZ *et al.* in [4]. The analysis is restricted to the small strain theory and to the plane strain condition.

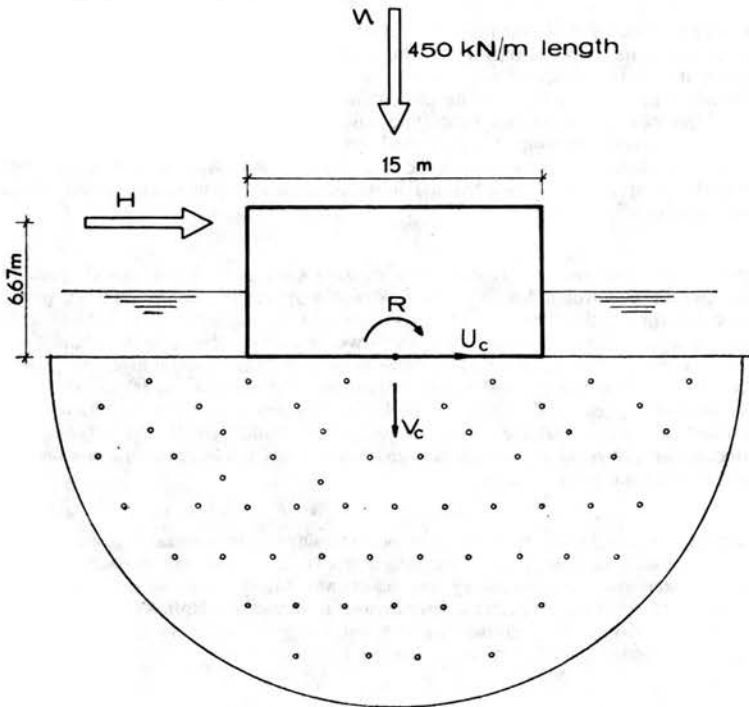


FIG. 1. In situ test on a caisson.

In Sect. 2 the geometry of the problem and the selection of the material constants are discussed. In Sect. 3 the numerical solution is presented in details and the results are compared with experimental measurements.

2. Geometry of the problem and the selection of material constants

Figures 1 and 2 present the geometry of the problem. The mesh of simple triangular elements with nine nodal variables was selected. The dimensions of the caisson and the point of application of the cyclic horizontal force are indicated in these figures. The boundary conditions were assumed as follows (see Fig. 2):

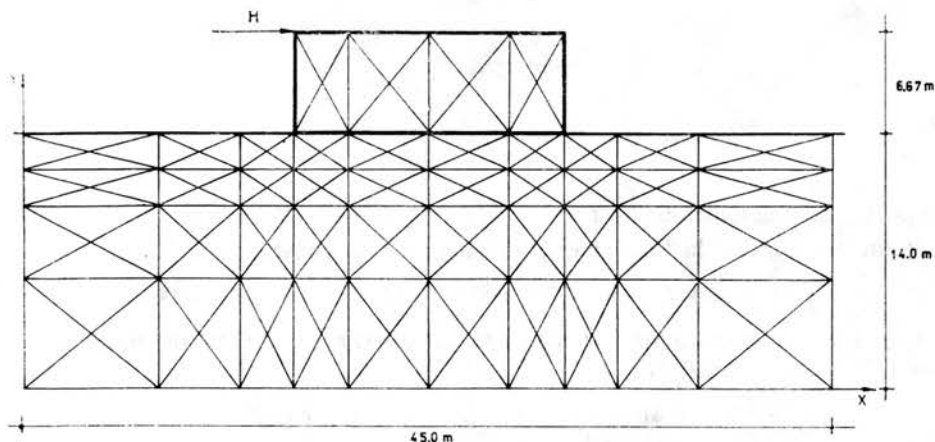


FIG. 2. Geometry of the problem.

- i) lower boundary: no vertical displacements, impermeable boundary,
- ii) left and right-hand side boundaries: no horizontal displacements, impermeable boundary,
- iii) upper boundary: no excess pore pressure i.e. full drainage (sec [6]).

The caisson was made of concrete. The length was about twice the width, thus the plane strain conditions were satisfied reasonably well. In the calculations it was assumed that the caisson behaves in an elastic manner and the proper elastic constants for concrete were selected. In fact, the strains in the caisson were negligible with respect to those in the soil.

The behaviour of soil skeleton was described by an elastoplastic double-hardening model discussed in details in [1]. It was assumed that the yield surface in the s, t plane is represented by three straight lines:

$$\begin{aligned}
 f_1 &= s - N(\epsilon_v^p) = 0, \\
 f_2 &= t - H(\epsilon_v^p, \epsilon_q^p) = 0, \\
 f_{cr} &= t - M_{cs}s = 0,
 \end{aligned}
 \tag{2.1}$$

where M_{cs} is a material constant and

$$\begin{aligned}
 t &= 1/2(\sigma_3 - \sigma_1) = \left[\left(\frac{\sigma_x - \sigma_y}{2} \right)^2 + \tau_{xy}^2 \right]^{1/2}, \\
 s &= -1/2(\sigma_3 + \sigma_1) = -1/2(\sigma_x + \sigma_y), \\
 \Delta \epsilon_v^p &= -(\Delta \epsilon_1^p + \Delta \epsilon_3^p); \quad \Delta \epsilon_q^p = \Delta \epsilon_3^p - \Delta \epsilon_1^p.
 \end{aligned}
 \tag{2.2}$$

The surface $f_1 = 0$ is the so-called volumetric yield surface. The surface $f_2 = 0$ is called shear yield surface and may be considered as the surface of the Tresca type. $f_{cr} = 0$ is the "failure" line and along this line a perfectly plastic behaviour satisfying the normality rule is assumed. The hardening functions $N(\epsilon_v^p)$ and $H(\epsilon_v^p, \epsilon_q^p)$ are proposed in the form

$$(2.3) \quad \begin{aligned} N(\varepsilon_v^p) &= \alpha(\varepsilon_v^p)^\beta, \\ H(\varepsilon_v^p, \varepsilon_q^p) &= t_{cr} \frac{\varepsilon_q^p}{a + \varepsilon_q^p}, \end{aligned}$$

where

$$t_{cr} = M_{cs} \alpha (\varepsilon_v^p)^\beta$$

and a , α , β are the material constants.

In the calculations the following set of constants was chosen:

$$\alpha = 7640 \text{ kgf/cm}^2, \quad \beta = 1.589, \quad M_{cs} = 0.6, \quad a = 0.0016.$$

Moreover, it was assumed that the elastic deformations are linear and the elastic constants were taken as

$$G = 120 \text{ kgf/cm}^2, \quad K = 400 \text{ kgf/cm}^2.$$

All these parameters were determined from the "triaxial" tests on drained material.

It should be noted that the identification of the model is very simple since both hardening functions (2.3) can be specified from two elementary tests.

According to the information obtained, the fraction of the pore volume occupied by air was of the order of 1%. Therefore the calculations were based on a somewhat compressible pore fluid. The compression modulus for the air-water mixture in pores was assumed as $K_p = 100 \text{ kgf/cm}^2$. Furthermore, the porosity of the soil n and the coefficient of permeability⁽¹⁾ k were taken as

$$n = 39\%, \quad k = 1.0 \cdot 10^{-4} \text{ m/s.}$$

3. Numerical results

The loading process of the soil mass was assumed to take place in three stages. First, the effective stresses due to the own weight of soil were generated. The initial stress state was assumed to be geostatic with the horizontal effective stresses equal to 1/2 of the vertical effective stresses. In the second stage the soil mass was loaded incrementally by a vertical force uniformly distributed along the bottom of the caisson. The total intensity of this loading corresponded to the weight of the caisson itself (450 kgf/cm). No pore pressures were generated and all displacements calculated in the next stage were determined with reference to this initial state.

Figure 3 presents the vertical displacement of the caisson's bottom as a function of its total weight, whereas Figs. 4a and 4b deal with the principal stress distribution after establishing of the caisson.

In the third stage the caisson was loaded by a cyclically varying horizontal force applied in series of time-steps. According to Fig. 5a, the loading process consisted of six portions with the constant amplitude, whereas each of them contained about 300 cycles. However, in the numerical process the time history of the loading was followed during only a few

(1) It was assumed that x , y are the principle directions of permeability and $k_x = k_y = k$.

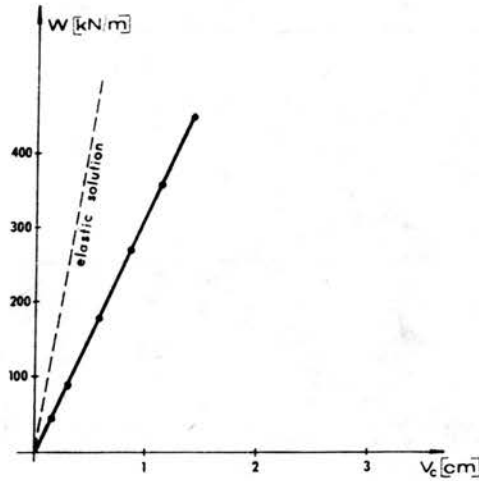
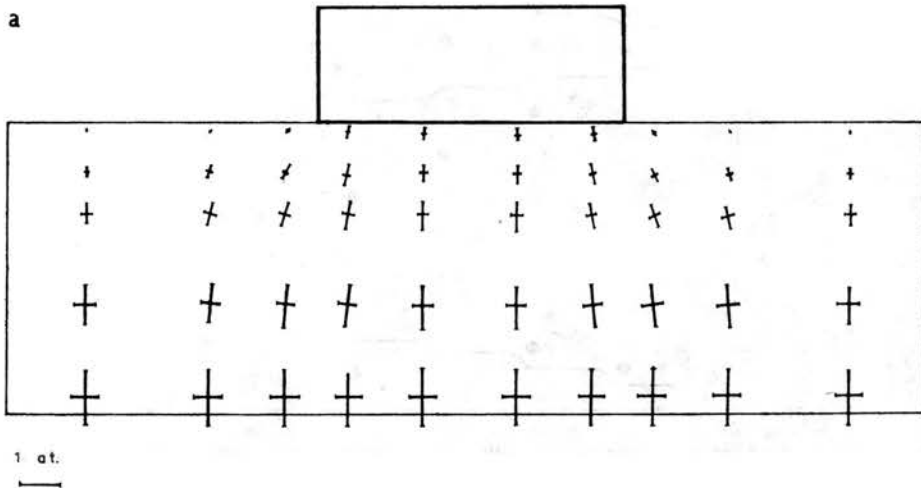


FIG. 3. Settlement of the caisson due to own weight.

cycles in each portion of the loading. It was observed that after about 3—4 cycles the plastic displacements of the caisson hardly increased and the soil behaviour was practically elastic (shakedown). Even such a simplified analysis proved to be time-consuming, requiring the application of many time-steps. For this reason the calculations were stopped when the solution for the 5th portion of the loading was already reached.

In each portion of loading the average horizontal force was first increased and then 3—4 loading cycles were followed. For each time-step both the pore water pressures and the displacement increments were calculated. Figures 5b and 6 present a comparison between the measured and predicted displacements of the caisson. Figure 5b shows the evolution of the displacement components as a function of time history, whereas Fig. 6 presents the final settlement of the caisson after the last cycle in the 5th loading portion.



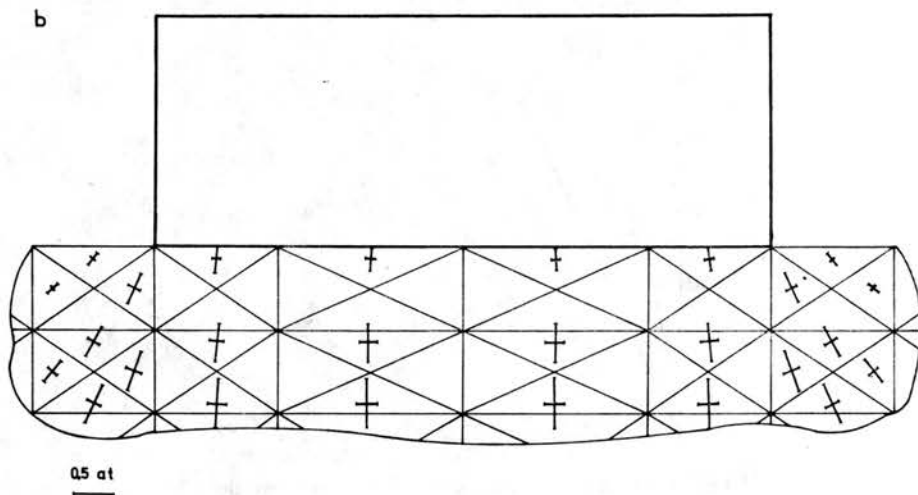


FIG. 4. Principal stresses distribution after establishing of the caisson: a) in the entire analysed region, b) at vicinity of the caisson.

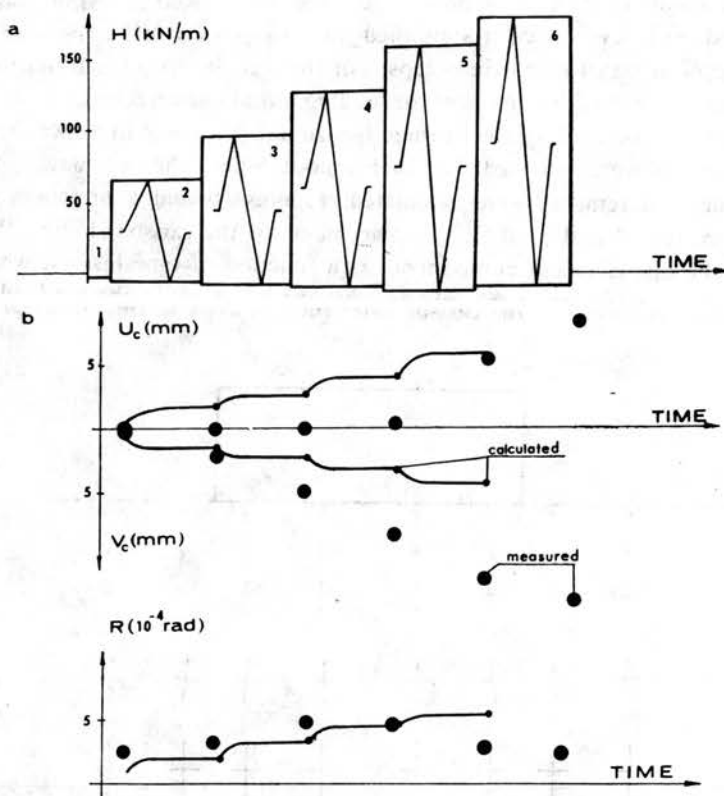


FIG. 5. a) Horizontal loading of the caisson plotted versus time, b) Settlement of the caisson at the end of each loading portion: Comparison between numerical and test results.

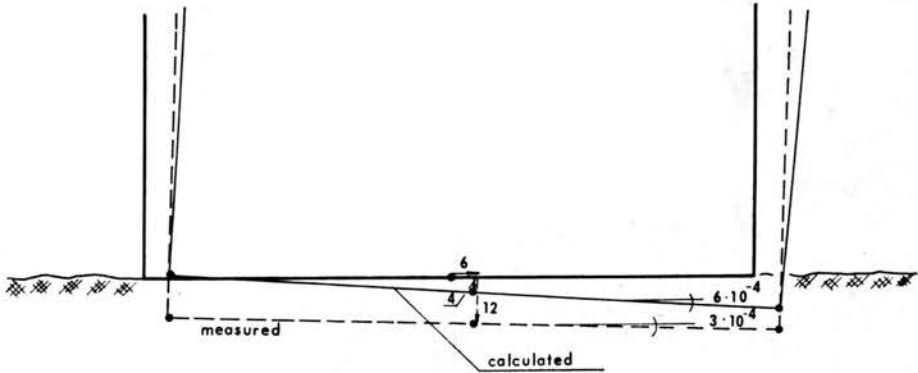


FIG. 6. Settlement of the caisson (mm) after last cycle in the 5th loading portion.

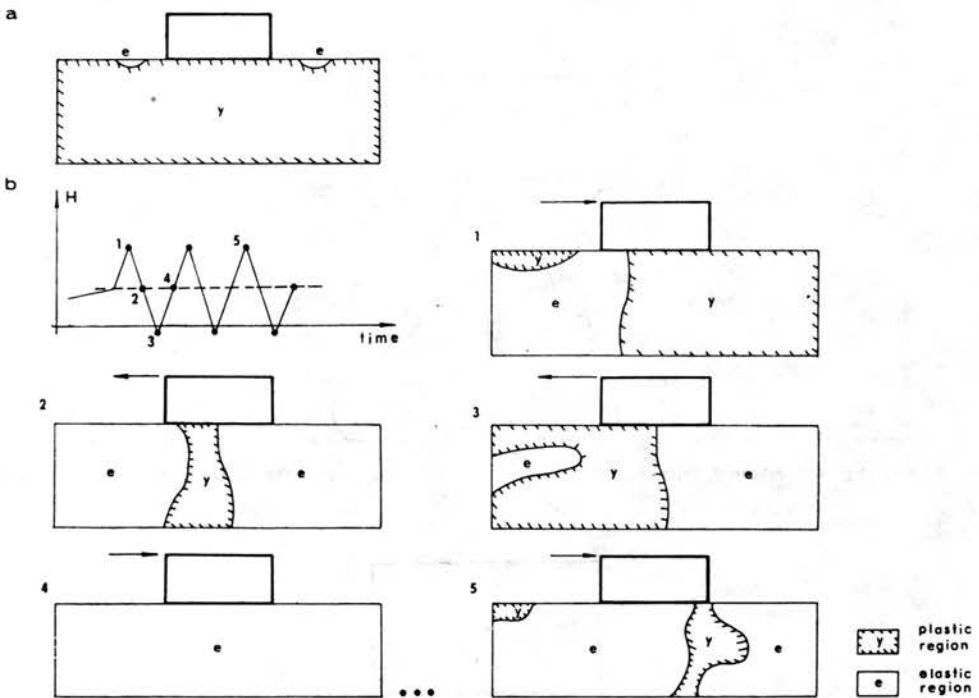


FIG. 7. Development of plastic zones in soil mass: a) due to own weight of the caisson, b) in the 2nd loading portion.

As it is seen from these figures the numerical prediction of the caisson settlement generally agreed with those obtained from experimental measurements. Calculated and measured, both the horizontal displacement and rotation of the caisson remain hardly different, only the vertical component seems to be numerically underestimated.

Let us describe now some more details of the numerical solution. Figure 7 presents the evolution of plastic zones in soil mass. According to the assumed hardening law, the plastic deformations developed right out at the beginning of the loading process. There-

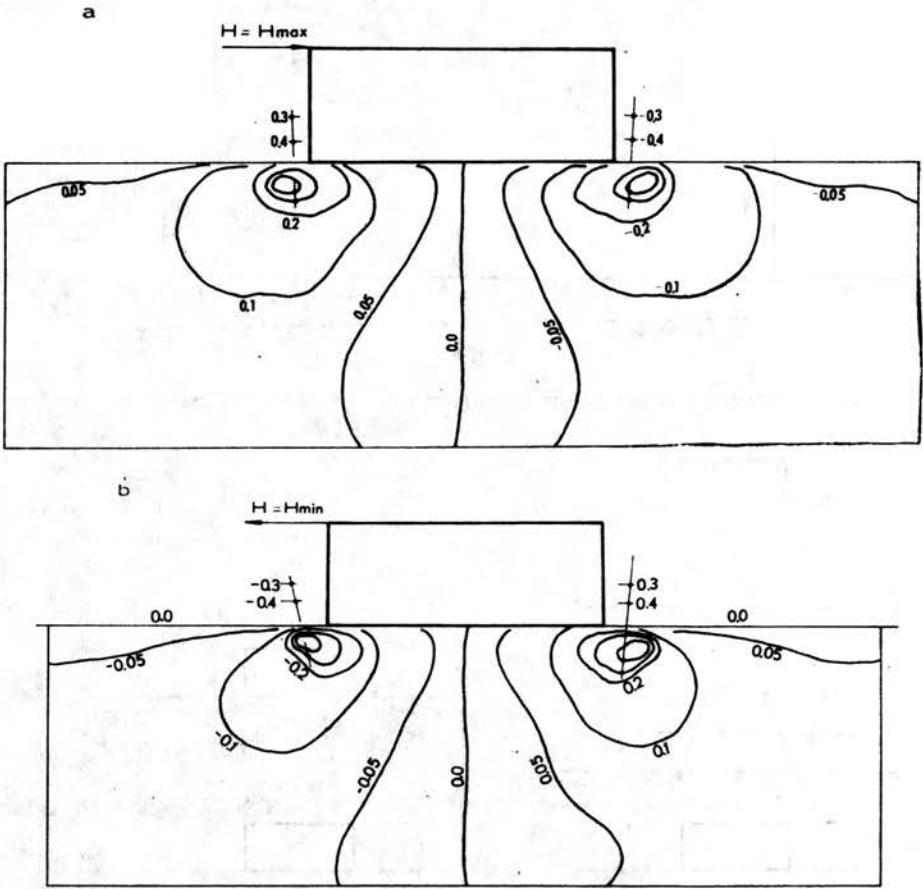


FIG. 8. Excess pore pressure distributions (m) at the end of 4th loading portion, a) $H = H_{max}$, b) $H = H_{min}$.

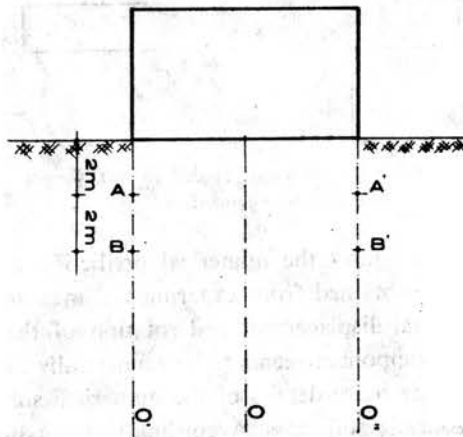


FIG. 9 Pore water pressure amplitudes (cm) at the end of 3rd and 4th loading portions.

Table 1. 3rd loading portion

measured	calculated	at	
33	40	<i>A</i>	} The average excess pore waterpressure ~ 0 (measured and calculated)
—	40	<i>A'</i>	
22	24	<i>B</i>	
20	24	<i>B'</i>	
0	0	„0” axis	

4th loading portion

measured	calculated	at	
47	57	<i>A</i>	} The average excess pore waterpressure ~ 0 (measured and calculated)
—	54	<i>A'</i>	
29	27	<i>B</i>	
26	26	<i>B'</i>	
0	0	„0” axis	

fore, the plastic zone due to the own weight of the caisson contained almost the whole analysed region of soil (Fig. 7a). The cyclic horizontal force caused a cyclically changeable distribution of plasticity regions. This situation, for the second loading portion, is presented in Fig. 7b. Here $H \equiv H_{\max}$ applied in the first cycle led to concentration of the plastic zone in a considerable part of the soil mass on the right-hand side of the caisson. Similarly, unloading of the caisson was associated with a remarkable concentration of plasticity. In fact, the whole first cycle caused significant irreversible changes in settlement of the caisson. However, in the course of following loading cycles the plastic zone gradually vanished and the displacement cycles were more and more purely elastic.

As it has been mentioned in the previous section, the calculations were based on a somewhat compressible pore fluid. This resulted in a quite good agreement between measured and predicted pore water pressure values due to cyclic loading. The distributions in Fig. 8 present the pore pressure excess for the 4th loading portion. In other portions such distributions were qualitatively similar to that in Fig. 8. Subsequently, Fig. 9 presents the amplitudes of the pore water pressure at the end of 3rd and 4th loading portions. The comparison with the measurements concerns the 0 axis and the points *A*, *B*, *B'*. It is worthy to note that both the numerical and experimental values are almost identical.

4. Final remarks

The similar boundary-value problem has already been considered for other models of soil skeleton behaviour ([2, 3]). A detailed comparison of all of these results is given in the doctor's thesis [6].

The application of an isotropic hardening model to the description of the soil skeleton seems to be justified. This follows from the fact that the vertical force corresponding to the weight of the caisson was much larger than the maximal amplitude of the horizontal force. Moreover, the loading scheme from Fig. 5a can be considered as one-way cyclic loading since the negative stroke can be disregarded with respect to the positive stroke.

The amplitudes of the pore pressure due to cyclic loading are predicted reasonably well. The assumption of a completely saturated soil with an incompressible pore fluid results in much larger pressures [2]. The conclusion is that the effect of the pore fluid compressibility is of importance and in many cases should not be neglected.

The computer program based on a three (or two) phase material and an elastoplastic soil skeleton seems to be sufficiently accurate for a realistic analysis of many engineering problems. Computation for dry soil is in fact a special option of such a program.

Acknowledgement

The author is indebted to ir. P. A. VERMEER and prof. A. VERRUIJT from the Delft University of Technology for their advice during the period in which this work was completed.

References

1. S. PIETRUSZCZAK, *Plane strain elastoplastic consolidation of soil by finite elements*, Part I, Arch. Mech., **32**, 2, 1981.
2. P. A. VERMEER, *A double hardening model for sand*, Geotechnique, **28**, 413-433, 1978.
3. C. I. KENTER, A. VERRUIJT, *Stability caissons Oosterschelde*, Soil mechanics laboratory of Delft, Report Co-40103-0, 1975.
4. O. C. ZIENKIEWICZ, S. VALLIAPAN, I. P. KING, *Elasto-plastic solutions of engineering problems, "Initial stress" finite element approach*, Int. Journ. Num. Meth. Eng., **4**, 579-582, 1972.
5. O. C. ZIENKIEWICZ, *The finite element method in engineering science*, Mc Graw-Hill, London 1977.
6. S. PIETRUSZCZAK, *Elastoplastic f.e. analysis of boundary-value problems in soil mechanics*, Doctoral Thesis [in Polish], IFTR Report 23/1979, Warszawa 1979.

POLISH ACADEMY OF SCIENCES
INSTITUTE OF FUNDAMENTAL TECHNOLOGICAL RESEARCH.

Received March 27, 1980.